Progress In Electromagnetics Research C, Vol. 59, 101–106, 2015

Bandpass Filters with Mixed Hairpin and Patch Resonators

Eugene A. Ogbodo*, Yi Wang, and Predrag Rapajic

Abstract—This paper presents a new implementation technique of transmission zeros in an in-line coupled filter. Neither cross couplings between non-adjacent resonators nor separate side-line resonators have been used. Instead a mixture of single-mode hairpin resonators and dual-mode patch resonators have been adopted in a bandpass filter with one asymmetric transmission zero. The introduction of the patch led to an improved frequency selectivity through an independently controllable transmission zero. This approach has been verified by a three-pole filter at 2.6 GHz with 8% bandwidth and a transmission zero at 2.4 GHz. Good agreement has been shown between the measurements and the simulation.

1. INTRODUCTION

Conventional planar bandpass filters (BPF) are usually formed of coupled-resonators of the same type for the ease of modelling and implementation. Increasingly more sophisticated filters composed of a mixture of different types of resonators have been proposed for various purposes. Some were intended to use non-uniform Q-factors across the resonators to better control the passband flatness in lossy filters [1]. Others used specific resonators for dual purpose such as in the case of integrated filter antennas, where the resonant antenna element serves as the radiator as well as one resonant pole in a filter [2, 3]. The resonant antenna element is usually of a completely different structure and characteristic from the other resonators.

This work explores the combined use of single-mode and dual-mode resonators in order to introduce transmission zeros in an in-line coupled filter without resorting to cross coupling between nonadjacent resonators or separate side-line resonators. The most widely used approach to generate transmission zeros is to implement multiple transmission paths within the filter by using coupling between non-adjacent resonators [4] and/or between the source and load [5]. This usually requires complicated topology of resonators for cross couplings. Extracted pole is another technique that has been used to realise transmission zeros but without cross coupling [6]. This usually involves resonators from the side-line coupled to the main in-line coupled resonators with the help of non-resonant and phase shifting structures [7–9]. In terms of physical implementation, for waveguide filters, side-line cavities could tap into the in-line cavities [7, 8]. For planar filters, microstrip resonators could be connected to the feedline with added phase shifting elements [9]. This paper presented a new implementation technique of transmission zeros in an in-line coupled filter.

A mixture of two hairpins and one patch resonator are used to produce a three-pole filter with one transmission zero. The three resonators are in-line coupled without any quadruplet or triplet structures for cross coupling, nor side-line resonators for extracted poles. The patch is used for its dual modes. One mode is coupled to the hairpins forming the transmission path, whereas the other orthogonal mode generates the transmission zero. Such a configuration is simple but significantly increases the selectivity of the filter. The patch also provides sufficient degrees of freedom to make the transmission zero controllable.

Received 29 July 2015, Accepted 18 September 2015, Scheduled 24 September 2015

* Corresponding author: Eugene Ogbodo (E.A.Ogbodo@greenwich.ac.uk).

The authors are with the Electrical, Electronic and Computer Engineering, University of Greenwich (Medway Campus), Kent, ME4 4TB, U.K..

2. DESIGN

2.1. Hairpin Three-Pole Bandpass Filter

The microstrip bandpass filter with mixed hairpin and patch resonators has been proposed to have the following specifications:

- Centre frequency of $f_{0,}$ 2.6 GHz.
- Passband return loss: 16 dB.
- Fractional Bandwidth (FBW): 8%.
- Transmission zero positioned at 2.4 GHz.

As a reference design for comparison, a conventional all-pole hairpin bandpass filter was first designed following the general filter implementation procedure. Using a passband ripple factor of 0.043 dB for a three-pole Chebyshev lowpass prototype, the g values were derived from [4] with $g_0 = g_4 = 1.0$, $g_1 = g_3 = 0.8516$ and $g_2 = 1.1032$. These were converted to the coupling parameters used for the physical dimensioning of the microstrip resonators as follows,

$$Q_{ex} = \frac{g_0 g_1}{FBW} \tag{1}$$

$$M_{12} = M_{23} = \frac{FBW}{\sqrt{g_1 g_2}} \tag{2}$$

where (1) givesthe input and output external quality factor whereas (2) is the coupling coefficient between adjacent resonators. $Q_{\text{ex}} = 10.645$, $M_{12} = M_{23} = 0.083$.

Full-wave simulations using CST Microwave Studio has been performed to find all the physical dimensions that provide the required coupling values. These values are extracted from the simulated S_{21} curves using the following equations [4].

$$Q_{ex} = \frac{f_0}{\Delta f} \tag{3}$$

$$M_{12} = M_{23} = \frac{f_2^2 - f_1^2}{f_2^2 + f_1^2} \tag{4}$$

These individual design steps resulted in the initial circuit layout, which was subject to further full-wave optimisation. Fig. 1(a) displays the conventional hair-pin filter and Table 1 lists the dimensions. The Roger RO3010 substrate is used for the design. The nominal dielectric constant is 11.2 and the loss tangent is 0.0023. The substrate is 1.27 mm thick.

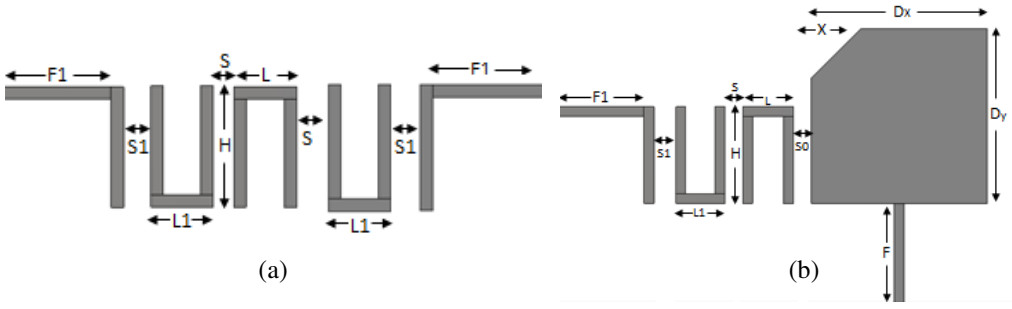

Figure 1. Circuit layouts of (a) the hairpin filter and (b) the hairpin-patch filter.

Table 1. Microstrip circuit dimensions in millimetre.

F	F_1	L	L_1	S	S_1	S_0	X	H	$D_x = D_y$
10	8.73	5.07	4.96	1.24	0.26	0.68	5	9.73	17.59

2.2. Square Patch Resonator and Mixed Hairpin-Patch Filter

To introduce a transmission zero in the three-pole filter without the complication of cross coupling or a separate side-line resonator for extracted poles, a dual-mode patch resonator is used in place of one of the hairpin resonator as shown in Fig. 1(b). The patch provides the orthogonal modes for the BPF, with one mode yielding the transmission path and the other yielding the transmission zero. The dimension of the required square resonator is estimated using $D = Dx = Dy = \lambda_{0g}/2$ and $\lambda_{0g} = c_0/f_0\sqrt{\varepsilon_r}$, where λ_{0g} is the guided-wavelength, c_0 is the speed of light, ε_r is the relative permittivity of 11.2, f_0 is the centre frequency of the filter, and D is the dimension of the square patch.

The square is simulated to resonate at 2.5 GHz. A chamfer X is then introduced to the square resonator; this allows the patch to split into two resonant frequencies. When $X = 5$ mm, the two frequencies generated were 2.45 GHz and 2.60 GHz. The eigen-mode solver in CST Microwave Studio has been used to study the resonant characteristics of the patch. Fig. 2 illustrates the simulated current distribution (phase = 90 deg for the plot) of the patch resonator with the arrows indicating the general direction of the currents. It is evident that the 2.45 GHz mode is orthogonal to the 2.6 GHz mode. From an equivalent circuit point of view, it is in parallel to the 2.6 GHz mode. The 2.60 GHz mode is coupled to the hairpin forming the transmission path. When the 2.45 GHz mode resonates, a stop band occurs creating the transmission zero.

In order to obtain the external quality factor (Q_{ex}) at the output of the patch, an arrangement was set up as shown in Fig. 3(a). At port-1, a 50 Ohm feeder line was tapped to the square patch resonator whereas the port 2 is weakly coupled to the square patch resonator. Using (3), the Q_{ex} of the square patch was obtained and calculated respectively. Fig. 3(b) illustrates the coupling arrangement used to calculate the coupling coefficient between the square patch and the adjacent resonator from (4). Fig. 1(b) and Table 1 show the circuit layout and dimensions after optimization, with the microstrip line width of 1.0 mm. Fig. 4 shows the simulated S-parameters of both the conventional hairpin filter

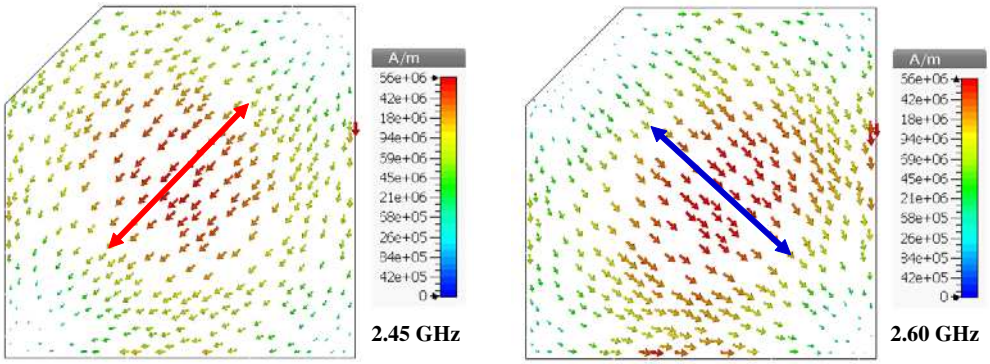

(a) (b)

Figure 2. Current distribution for the orthogonal modes of the patch resonator. $D_x = D_y = 18$ mm, $X = 5$ mm.

(a) (b)

Figure 3. (a) Arrangement for extracting Q_{ex}; (b) Arrangement for extracting coupling coefficients.

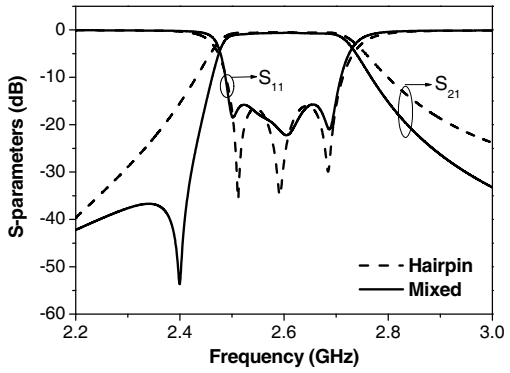

Figure 4. The simulated responses of the mixed hairpin-patch filter in comparison with a conventional hairpin filter of the same order.

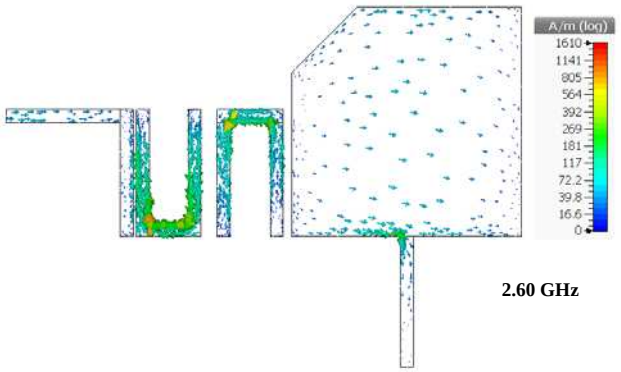

Figure 5. Simulated surface current distribution of the hairpin-patch filter at 2.60 GHz.

and the hairpin-patch filter, which clearly exhibits a transmission zero at 2.4 GHz. Fig. 5 illustrates the simulated current distribution (phase = 90° for the plot) on the mixed resonator filter at 2.6 GHz.

It has to be said that, in the design of the hairpin-patch filter, the coupling matrix was not extracted to represent the required frequency response with the prescribed transmission zero. The physical dimensioning of the hairpin-patch filter was guided by the conventional hairpin filter and its responses. After replacing the last resonator in Fig. 1(a) by the patch, parameter studies and optimizations have been used to achieve the required passband return loss and the transmission zero. The feedline to the first hairpin resonator as well as the first two hairpins are kept unchanged. The main dimensions that have been optimized include the size of the patch, the chamfers, and the tapping point of the feed line at the patch.

3. PARAMETER STUDY

The parameter study mainly looked into the effect of the chamfers in the patch. Two chamfers (X and Xc) are shown in Fig. 6(a). The chamfer X determines the lower mode at around 2.6 GHz. Fig. 6(b) illustrates the change of response as a function of the chamfer X. As the chamfer also controls the coupling between the two orthogonal modes of the patch, the overall bandwidth has been affected. The transmission zero is also shifted slightly as a result. The more effective way to change the transmission zero is to alter the longer diagonal path, as indicated in Fig. 2(a), in the patch. This can be achieved by introducing the chamfer Xc as shown in Fig. 6(a), or an extension stub if the transmission zero frequency were to be lowered. From Fig. 6(c), it can be seen that the increase of Xc pushes the transmission zero to higher frequency but hardly affects the upper edge of the passband. In the case of the filter for Figs. 1 and 4 with the transmission zero at 2.4 GHz, this chamfer Xc is not required. The size of the patch (D_x and D_y), the tapping point of the feedline to the patch and the coupling between the patch and the hairpin are other parameters that can be adjusted in optimization. If more degrees of freedom are required, stubs or slots can be added onto the patch.

It should also be noted that Xc not only shifts the transmission zero but also degrades it and affects the passband. This is because the chamfer Xc also impacts on the coupling between the two patch modes. After shifting the transmission zero, further optimisation of other parameters such as the size of the patch and the coupling between the patch and the hairpin is required to restore the passband.

4. FABRICATION AND MEASUREMENTS

The circuit is fabricated with the milling method using the LPKF ProtoMat S63 circuit board plotter. To prevent radiation loss and preserve the high Q-factor of the patch, the circuit is housed in a metalised box. Fig. 7 shows the fabricated device and Table 1 provides the microstrip circuit dimensions in

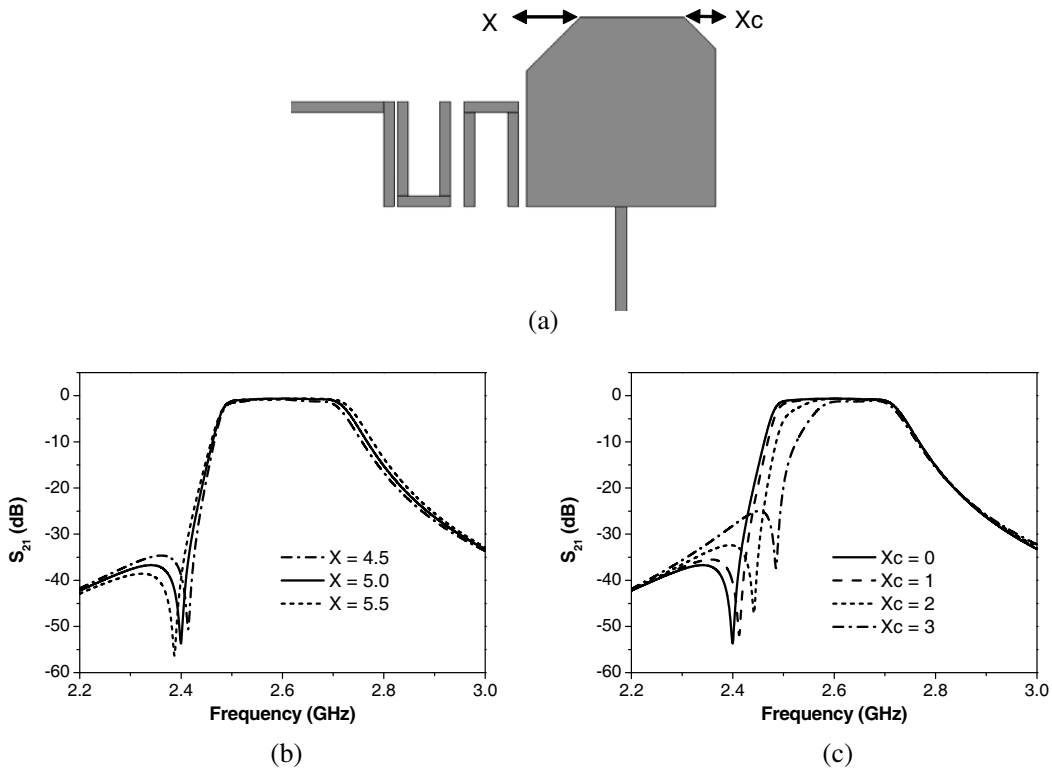

Figure 6. Parameter studies. (a) The chamfers X and Xc; (b) The change of S_{21} with X; (c) The change of S_{21} with Xc.

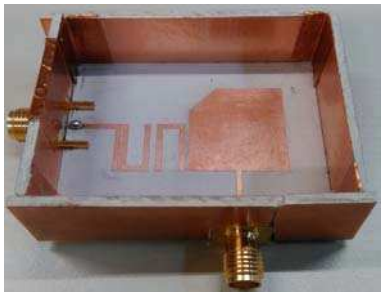

Figure 7. Photo of the fabricated filter with its box lid removed.

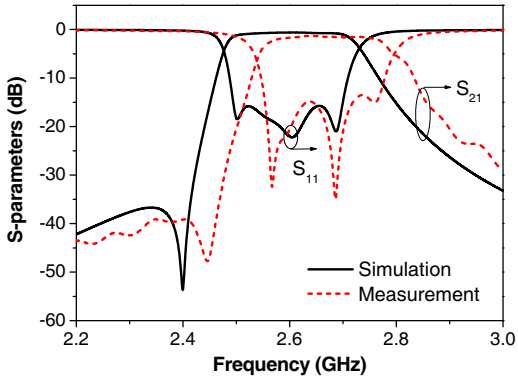

Figure 8. Simulated and measured responses of the hairpin-patch filter.

millimetre. Agilent Network Analyser N5230A was used to measure the fabricated device. A comparison between the simulated and measured results is shown in Fig. 8. It can be seen that a reasonablely good agreement has been achieved. The transmission zero can be identified at 2.446 GHz. There is a significant shift of the measured responses to higher frequency by nearly 50 MHz. This is mainly due to the over-milling of the circuit when the parameters of the milling machine are not optimised to process the ceramic-filled Roger RO3010 substrate. The minimum measured insertion loss in the passband is 1.3 dB and the return loss is better than 13 dB.

5. CONCLUSION

A dual-mode patch resonator was used to replace one hairpin resonator in a three-pole hairpin bandpass filter. One of the dual modes is coupled to the filter to generate the third pole required for the filter while the other mode is used in generating the transmission zero. This combination resulted in improved frequency selectivity in the bandpass filter as compared with the conventional hairpin filter. The parameter studies have demonstrated the controllability of the transmission zero as well we the bandwidth of the mixed hairpin-patch filter. The circuit layout taken in actualizing this proposed design is relatively straight forward. It eliminates the need of cross coupling between non-adjacent resonators and presents a new way to implement the extracted pole. This leads to the possibility of integrating the dual-mode patch into other filtering networks such as diplexers and multiplexers, where reduced complexity in the resonator topology is highly desired. One challenge in the design and optimisation is the interdependence of the filter responses on multiple parameters in relationship to the patch resonator. Although a shielded patch resonator is desired for its higher Q than a microstrip resonator, the requirement for metal shielding is a limitation when the device form factor is the main design drive. Similar design concept can be employed using microstrip resonators that do not pose problems with radiation losses.

REFERENCES

1. Meng, M. and I. Hunter, "The design of parallel connected filter networks with non-uniform Q resonators," *IEEE MTT-S Int. Microw. Symp. Dig.*, Vol. 61, No. 1, 372–381, June 17–22, 2012.
2. Yusuf, Y. and X. Gong, "Compact low-loss integration of high-3-D filters with highly efficient antennas," *IEEE Trans. Microw. Theo. Techn.*, Vol. 59, No. 4, 857–865, April 2011.
3. Mao, C. X., S. Gao, Z. P. Wang, Y. Wang, F. Qin, B. Sanz-Izquierdo, and Q. X. Chu, "Integrated filtering-antenna with controllable frequency bandwidth," *9th Europ. Conf. on Antennas and Propagation (EuCAP)*, April 12–17, 2015.
4. Hong, J.-S., *Microstrip Filters for RF/Microwave Applications*, John Wiley & Sons, Inc., 2011.
5. Liao, C. and C. Chang, "Design of microstrip quadruplet filters with source-load coupling," *IEEE Trans. Microwave Theory and Techniques*, Vol. 53, No. 7, 2302, 2308, July 2005.
6. Rhodes, J. and R. Cameron, "General extracted pole synthesis technique with applications to low-loss TE_{011} mode filters," *IEEE Trans. Microwave Theory and Techniques*, Vol. 28, No. 9, 1018–1028, September 1980.
7. Macchiarella, G. and M. Politi, "Use of generalized coupling coefficients in the design of extracted-poles waveguide filters with non-resonating nodes," *IEEE MTT-S Int. Microw. Symp. Dig.*, 1341–1344, June 2009.
8. Jedrzejewski, A., N. Leszczynska, L. Szydlowski, and M. Mrozowski, "Zero-pole approach to computer aided design of in-line SIW filters with transmission zeros," *Progress In Electromagnetics Research*, Vol. 131, 517–533, 2012.
9. Yeo, K., M. Lancaster, and J. Hong, "The design of microstrip six-pole quasi-elliptic filter with linear phase response using extracted-pole technique," *IEEE Trans. Microwave Theory and Technique*, Vol. 40, No. 2, 321–327, 2001.